

Ionization of Xenon Rydberg Atoms at a Metal Surface

S. B. Hill, C. B. Haich, Z. Zhou, P. Nordlander, and F. B. Dunning

Department of Physics and Astronomy and the Rice Quantum Institute, Rice University, P.O. Box 1892, Houston, Texas 77251
(Received 5 July 2000)

Experiments in which a thermal-energy beam of xenon Rydberg atoms is directed at near grazing incidence onto a flat Au(111) surface are described that provide new insight into charge transfer and electron tunneling during atom/surface interactions. Analysis of the data shows that for the present range of principal quantum number n , $13 \leq n \leq 20$, ionization occurs at an atom/surface separation $Z_i = (4.5 \pm 0.9)n^2 a_0$, where $n^2 a_0$ is the Bohr radius of the atom. This result is in good agreement with the value $Z_i \sim 3.8n^2 a_0$ predicted by *ab initio* hydrogenic theory.

PACS numbers: 79.20.Rf, 34.50.Dy

Because of their large physical size and weak binding, Rydberg atoms are strongly perturbed by nearby metal surfaces and thus provide a particularly sensitive probe of atom/surface interactions. Even relatively far from the surface, the motion of the excited electron is influenced by image charge interactions which shift the atomic energy levels and distort the electronic wave functions. Furthermore, ionization can occur through resonant tunneling of the excited electron into a vacant level in the metal which causes the states to become very broad close to the surface. Despite this rather extreme behavior, relatively few studies of Rydberg atom/surface interactions have been reported. Theoretical work has focused on hydrogen Rydberg atoms, initially using perturbation methods [1] and, more recently, the complex scaling and the time-dependent close-coupling techniques [2–4]. Theory shows that, as the surface is approached, the degeneracy of the (hydrogenic) levels is lifted through formation of hybridized, “Stark-like” states. The electron probability density for some hybridized states is maximal towards the surface, others towards vacuum. The predicted tunneling rates vary widely from state to state and are many orders of magnitude greater for states oriented toward the surface. The first experimental estimate of the atom/surface separation at which ionization occurs, i.e., the ionization distance, was obtained by measuring the transmission of $\text{Na}(nd)$ Rydberg atoms through micrometer-sized slits [5]. However, subsequent experiments using fine-mesh grids and lithium Rydberg atoms suggested that transmission might also be affected by localized electric fields produced by adsorbed surface layers [6]. The first direct observation of ions produced through surface ionization was made by directing $\text{K}(nd)$ Rydberg atoms at near-grazing incidence onto a gold surface [7]. However, potassium deposition on the surface again complicated the interpretation of the data. In the present work we have eliminated these earlier problems by studying the ionization of Xe Rydberg atoms incident under clean UHV conditions on a flat Au(111) surface. The use of Xe atoms, which do not stick to or react chemically with the target surface, allows measurements under stable well-defined conditions. Efficient surface ionization is observed. The measured ionization distances scale as

$\sim n^2$, i.e., approximately as the atomic radius, and are in good agreement with those predicted by *ab initio* hydrogenic theory.

In the present work, xenon Rydberg atoms are directed at near-grazing incidence onto the target surface. Ions formed by tunneling are attracted to the surface by the electric fields associated with their image charges. These fields are large and will rapidly accelerate an ion to the surface where it will be neutralized by an Auger process. To prevent this, an external electric field is applied perpendicular to the surface. Because the initial image charge field experienced by an ion, and thus the external field required to counteract it, depends on the distance from the surface at which ionization occurs, the ionization distance can be inferred from measurements of the surface ionization signal as a function of applied field.

The present apparatus is shown schematically in Fig. 1. Xenon Rydberg atoms are created by photoexciting the 3P_0 atoms in a mixed $\text{Xe}(^3P_{0,2})$ metastable atom beam that is produced by electron impact excitation of ground-state xenon atoms contained in a supersonic expansion, as described elsewhere [8]. The beam is tightly collimated by an 80- μm -wide aperture before striking the surface

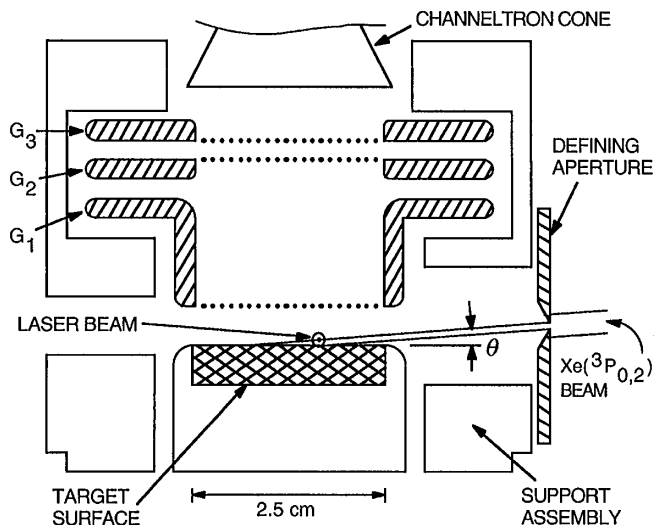


FIG. 1. Schematic diagram of the experimental apparatus.

[9] to obtain a well-defined angle of incidence $\theta \sim 4^\circ$. The 3P_0 atoms are excited using the crossed output of a UV-pumped Coherent CR899-21 C-47 dye laser. The laser beam is focused to a diameter of $\sim 100 \mu\text{m}$ to match the $\text{Xe}(^3P_{0,2})$ beamwidth. The Rydberg atoms are created close to the target surface to ensure that the majority of them will reach the surface before decaying. The experiments are conducted in a pulsed mode by forming the output of the laser into a train of pulses of $\sim 1 \mu\text{sec}$ duration and $\sim 5 \text{ kHz}$ repetition frequency using an acousto-optic modulator. Excitation occurs in a relatively weak dc field, $\sim 60\text{--}510 \text{ V cm}^{-1}$, produced by application of a positive bias to the target surface. (The opposing fine-mesh grids G_1 and G_2 are held at ground potential.) The presence of the dc field allows selective excitation of “red” or “blue” Stark states for which the electron probability density is maximal towards or away from the surface, respectively. In this work, the laser frequency and polarization are selected to excite the reddest $m = 0$ state in each $\text{Xe}(n)$ Stark manifold. Approximately $0.1 \mu\text{s}$ after the laser pulse, a large rectangular voltage pulse with $\sim 0.1 \mu\text{s}$ rise time and $\sim 10 \mu\text{s}$ duration is applied to the target surface to establish a strong ion-collection field. Ions that escape the surface are accelerated to a bell-mounted channeltron for detection. Grid G_3 and the entrance cone of the channeltron are held at -2.5 kV . The ion impact energy at the channeltron is governed by the potential difference between the channeltron cone and the target surface and, therefore, varies with target bias. This leads to small ($<20\%$) changes in ion detection efficiency that are corrected for in the data presented here.

A typical ion arrival time distribution is shown in the inset in Fig. 2. A broad feature is observed whose temporal

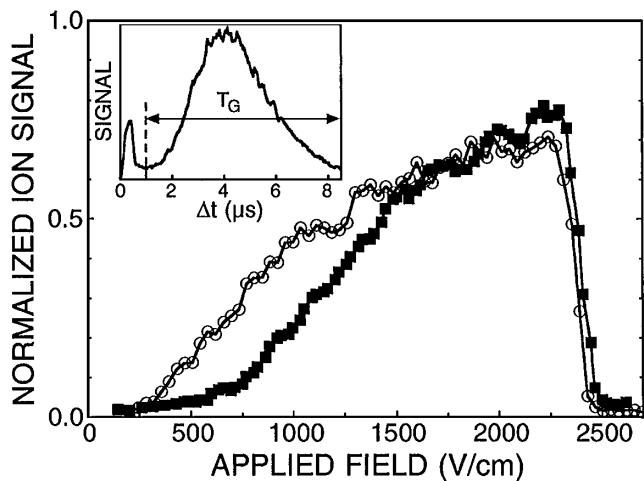


FIG. 2. Applied field dependence of the surface ion signals measured for $\text{Xe}(n = 20)$ atoms incident on the Au(111) surface (■) and the copper mirror (○). The data are normalized to total Rydberg atom production. The inset shows a typical ion arrival time distribution at the detector and the time gate T_G used to discriminate against ions produced by blackbody photoionization.

location and width are consistent with the expected Rydberg atom flight times to the surface. The small peak at early times is attributed to ions produced by blackbody-radiation-induced photoionization during the laser pulse [10]. To discriminate against these ions, a time gate T_G , indicated on the inset, is used to count only those ions detected at times consistent with formation in an atom/surface interaction. If tunneling occurs at an atom/surface separation Z_i , the minimum external field (in a.u.) that must be applied to prevent an ion from striking the surface and being lost is [3]

$$E_{\min}(Z_i, T_{\perp}) = \left[\frac{1}{2Z_i} + \sqrt{\frac{T_{\perp}}{Z_i}} \right]^2, \quad (1)$$

where $T_{\perp} = mv_{\perp}^2/2$ is the kinetic energy perpendicular to the surface at the time of ionization. Thus by measuring the ion signal as a function of applied field, E_{\min} and, hence, Z_i can be determined.

Figure 2 shows the applied field dependence of the surface ion signal observed when $\text{Xe}(n = 20)$ atoms are incident on a flat Au(111) surface. The data are normalized to the initial number of Rydberg atoms created, which was determined by field ionization. For sufficiently large applied fields, the majority of these atoms are detected through surface ionization. This indicates that only a small fraction of the Rydberg atoms decay prior to reaching the surface and demonstrates that surface ionization can provide an efficient means to detect Rydberg atoms. The sudden decrease in the surface ion signal at large applied fields is due to direct field ionization of the Rydberg atoms. This occurs as the field is applied, producing ions that arrive at the detector prior to the time gate and that are therefore not counted. Figure 2 also includes data obtained using a (diamond-turned) copper mirror as the target surface. Efficient surface ionization is again observed but, surprisingly, the threshold field for ion detection is significantly smaller than for the Au(111) surface. (A similar reduction in threshold field was observed at other n .) Atomic force microscopy indicates that this difference may be explained by the different topographies of the two surfaces. The Au(111) surface, which was prepared by epitaxial growth of a 150-nm-thick film on a cleaved mica substrate, is close to atomically flat, whereas the mirror surface has appreciable roughness with variations in height of as much as 40 nm over a lateral distance of $2 \mu\text{m}$. Such surface irregularities result in a range of effective incidence angles which can decrease and, for some trajectories, even change the sign of the T_{\perp} term in Eq. (1) thereby lowering the threshold field. Also, surface roughness can lead to local field inhomogeneities at the surface which can further lower the apparent threshold fields. Sensitivity to surface roughness may account, in part, for the low thresholds observed in the earlier studies using $K(nd)$ Rydberg atoms [7].

The observed onset in the surface ionization signal from the Au(111) surface is shown in Fig. 3(a) for several values

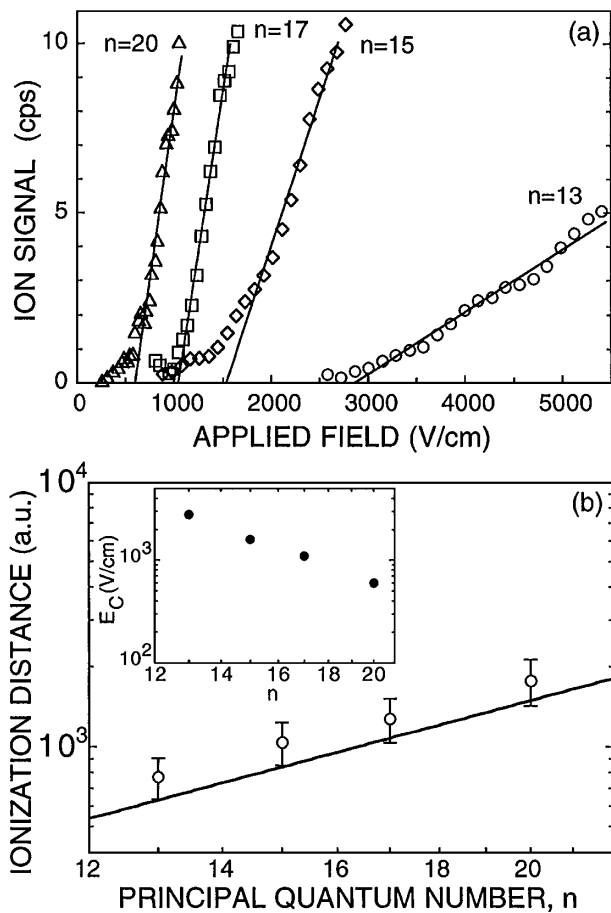


FIG. 3. (a) Measured onset of the surface ionization signal for several values of n . The critical threshold fields are plotted versus n in the inset in (b). (b) n dependence of the inferred ionization distance Z_i . Open circles with error bars, experimental data; —, predictions of hydrogenic theory.

of n . The critical threshold fields E_c were estimated using the indicated simple straight-line fits to the data and are plotted versus n in the inset in Fig. 3(b). The measured threshold fields are used in Eq. (1) with the value $v_{\perp} = 1.6 \times 10^3 \text{ cm s}^{-1}$ that encompasses the lowest 10% of the anticipated Rydberg atom velocity distribution to determine the corresponding ionization distances Z_i , which are plotted in Fig. 3(b). The error bars reflect the uncertainties in the angle of incidence ($\pm 1^\circ$), the atom velocity ($\pm 25\%$), and the interpolated threshold field ($\pm 15\%$). The ionization distances scale with the physical size of the atoms according to $Z_i = (4.5 \pm 0.9)n^2 a_0$, where $n^2 a_0$ is the Bohr radius. Since the initial image charge field experienced by an ion varies as Z_i^{-2} , this accounts for the observed n^{-4} scaling in threshold field [see the inset in Fig. 3(b)]. Interestingly, for the present θ and the same ionization distance Z_i , Eq. (1) predicts that atoms with velocities in the upper 10% of the velocity distribution require collection fields $\sim 40\%$ greater than the measured threshold E_c . The distribution of atom velocities can thus account, in part, for the lack of a “steplike” increase in ion

signal at threshold. However, effects associated with mixing of neighboring Stark states might also be important.

Figure 3(b) includes ionization distances predicted by hydrogenic complex scaling calculations that include the presence of the external field [3]. Calculated widths for the reddest, most strongly surface oriented $m = 0$ $H(n = 13)$ Stark state are shown in Fig. 4 as a function of atom/surface separation Z for several values of applied field. For a given Z , the width increases dramatically with applied field due to the strong polarization of the atom which increases the electron probability density near the surface and facilitates tunneling. This strong polarization of the atoms is illustrated by the calculated electron probability density shown in the inset in Fig. 4. Calculations in which the predicted ionization rate is integrated along the incident atom trajectory for the measured threshold fields suggest that ionization should occur at $Z_i \sim 3.8n^2 a_0$ [11]. Because the width of the states increases exponentially with decreasing atom/surface separation, this value is not particularly sensitive to atom velocity or angle of incidence. Indeed, for atoms incident normally, ionization would occur at $Z \sim 3.3n^2 a_0$. (The field required to collect the ions, however, would be more than an order of magnitude larger because of the large increase in v_{\perp} .) The theoretical prediction is in good agreement with the measured values given that the theory uses an *ab initio* hydrogenic model with no adjustable parameters. In fact, the ionization distances for xenon are expected to be larger because the polarization potential associated with the Xe^+ core should enhance tunneling [12].

The present work demonstrates that Rydberg atoms provide a powerful probe of image charge effects and charge transfer during atom/surface interactions. Further studies

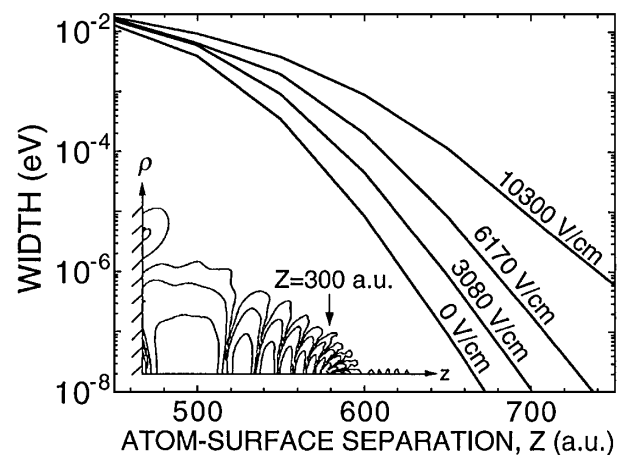


FIG. 4. Calculated widths for the reddest, most strongly surface oriented $m = 0$ $H(n = 13)$ Stark state as a function of atom/surface separation Z for the values of applied field indicated. For reference, the inset shows a contour plot of the electron probability density [3] $|\psi(\rho, z)|^2$ for the corresponding $m = 0$ $H(n = 10)$ state for $Z = 300$ a.u. and a field of 500 V cm^{-1} . The probability density varies by an order of magnitude between neighboring contours.

at conducting surfaces using different Stark states (to control the initial orientation of the electron wave function) and different angles of incidence (to vary v_{\perp}), coupled with further theoretical calculations, promise new insights into the behavior of atoms near a surface and into electron tunneling. These processes can be further explored by measurements using narrow-electronic-band-gap dielectrics. If the bottom of the conduction band lies below the vacuum level, tunneling is again possible but the image charge fields are reduced relative to those at a conducting surface by a factor $(\xi - 1)/(\xi + 1)$, where ξ is the dielectric constant. Studies of very thin (1–10 nm) conducting films grown epitaxially on insulating substrates are also of interest because for such films quantum size effects become important and influence the tunneling process. Recent calculations [13] point to large variations in ionization distance with film thickness and suggest that Rydberg atoms will be a particularly sensitive probe of quantum size effects.

This research was supported by the National Science Foundation and the Robert A. Welch Foundation.

-
- [1] A. V. Chaplik, Zh. Eksp. Teor. Fiz. **54**, 332 (1968) [Sov. Phys. JETP **27**, 178 (1968)].
 [2] P. Nordlander, Phys. Rev. B **53**, 4125 (1996).
 [3] P. Nordlander and F. B. Dunning, Phys. Rev. B **53**, 8083

- (1996); Nucl. Instrum. Methods Phys. Res., Sect. B **125**, 300 (1997).
 [4] P. Kürpick, U. Thumm, and U. Wille, Phys. Rev. A **57**, 1920 (1998).
 [5] C. Fabre, M. Gross, J. M. Raimond, and S. Haroche, J. Phys. B **16**, L671 (1983).
 [6] C. A. Kocher and C. R. Taylor, Phys. Lett. A **124**, 68 (1987).
 [7] D. F. Gray, Z. Zheng, K. A. Smith, and F. B. Dunning, Phys. Rev. A **38**, 1601 (1988).
 [8] S. B. Hill, C. A. Haich, F. B. Dunning, G. K. Walters, J. J. McClelland, R. J. Celotta, and H. G. Craighead, Appl. Phys. Lett. **74**, 2239 (1999).
 [9] Like Rydberg atoms, metastable atoms undergo ionization through resonant tunneling as they approach the surface, but at a much smaller atom/surface separation. Tests, however, revealed that the product Xe^+ ions were efficiently neutralized at the surface and did not leave the surface either as ions or highly excited neutral atoms.
 [10] W. P. Spencer, A. G. Vaidyanathan, D. Kleppner, and T. Ducas, Phys. Rev. A **26**, 1490 (1982).
 [11] The simple “over-the-barrier” model [J. Burgdörfer, P. Lerner, and F. W. Meyer, Phys. Rev. A **44**, 5674 (1991)] predicts ionization at $Z_i \sim 3n^2 a_0$.
 [12] J. Brau and P. Nordlander, Surf. Sci. **448**, L193 (2000); D. Teillet-Billy, J.-P. Gauyacq, and P. Nordlander, Surf. Sci. **371**, L235 (1997).
 [13] B. Bahrim, P. Kürpick, U. Thumm, and U. Wille, Nucl. Instrum. Methods Phys. Res., Sect. B **164–165**, 614 (2000); U. Thumm, P. Kürpick, and U. Wille, Phys. Rev. B **61**, 3067 (2000).